
Research Article: New Research | Neuronal Excitability

Spontaneous Infralow Fluctuations Modulate Hippocampal EPSP-PS Coupling

Michael B. Dash^{1,2}, S. Ajayi², L. Folsom², P.e. Gold² and D.I. Korol²

¹Department of Psychology, Middlebury College, Middlebury, VT 05753

²Department of Biology, Syracuse University, Syracuse, NY 13244

DOI: 10.1523/ENEURO.0403-17.2017

Received: 25 November 2017

Accepted: 15 December 2017

Published: 8 January 2018

Author contributions: M.B.D., P.E.G., and D.K. designed research; M.B.D., S.A., and L.F. performed research; M.B.D., S.A., and L.F. analyzed data; M.B.D., P.E.G., and D.K. wrote the paper.

Funding: <http://doi.org/10.13039/100000001>National Science Foundation (NSF)
IOS 0843175
IOS 1318490

Funding: <http://doi.org/10.13039/100000002>HHS | National Institutes of Health (NIH)
P50 AT006268

Funding: Syracuse University Center for Aging and Policy Studies
NIA P30 AG034464

The authors declare no competing financial interests.

Supported by NSF IOS 0843175 and 1318490, NIH P50 AT006268 from ODS, NCAAM, and NCI, and the Syracuse University Center for Aging and Policy Studies (NIA P30 AG034464).

Corresponding author: Michael Dash, Department of Psychology, 281 McCardell Bicentennial Hall, 276 Bicentennial Way, Middlebury College, Middlebury, VT 05753. mdash@middlebury.edu

Cite as: eNeuro 2018; 10.1523/ENEURO.0403-17.2017

Alerts: Sign up at eneuro.org/alerts to receive customized email alerts when the fully formatted version of this article is published.

Accepted manuscripts are peer-reviewed but have not been through the copyediting, formatting, or proofreading process.

Copyright © 2018 Dash et al.

This is an open-access article distributed under the terms of the Creative Commons Attribution 4.0 International license, which permits unrestricted use, distribution and reproduction in any medium provided that the original work is properly attributed.

1 SPONTANEOUS INFRASLOW FLUCTUATIONS MODULATE
2 HIPPOCAMPAL EPSP-PS COUPLING
3

4 M.B. Dash^{1,2}, S. Ajayi², L. Folsom², P.E. Gold², and D.L. Korol²

5 ¹Department of Psychology, Middlebury College, Middlebury, VT 05753

6 ²Department of Biology, Syracuse University, Syracuse, NY 13244
7

8 Abbreviated title: Infraslow SBA modulates EPSP-PS coupling
9

10 Corresponding author:

11 Dr. Michael Dash
12 Department of Psychology
13 281 McCardell Bicentennial Hall
14 276 Bicentennial Way
15 Middlebury College
16 Middlebury, VT 05753
17 mdash@middlebury.edu

18
19 Pages (39), Figures (6), Tables/Multimedia/Models (0), Abstract Words (211),
20 Introduction Words (613), Discussion Words (1691).
21

22
23 Acknowledgements: Supported by NSF IOS 0843175 and 1318490, NIH P50 AT006268
24 from ODS, NCAAM, and NCI, and the Syracuse University Center for Aging and Policy
25 Studies (NIA P30 AG034464). The authors declare no competing financial interests.

26 **Abstract**

27 Extensive trial-to-trial variability is a hallmark of most behavioral, cognitive, and
28 physiological processes. Spontaneous brain activity (SBA), a ubiquitous phenomenon
29 that coordinates levels and patterns of neuronal activity throughout the brain, may
30 contribute to this variability by dynamically altering neuronal excitability. In freely-
31 behaving male rats, we observed extensive variability of the hippocampal evoked
32 response across 28-min recording periods despite maintaining constant stimulation
33 parameters of the medial perforant path. This variability was related to antecedent
34 SBA: increases in low (0.5-9Hz), and high (40.25-100Hz), frequency band-limited power
35 (BLP) in the 4s preceding stimulation were associated with decreased slope of the field
36 excitatory postsynaptic potential (fEPSP) and increased population spike (PS)
37 amplitude. These fluctuations in SBA and evoked response magnitude did not appear
38 stochastic, but rather exhibited coordinated activity across infraslow timescales (0.005-
39 0.02Hz). Specifically, infraslow fluctuations in high and low frequency BLP were
40 antiphase with changes in fEPSP slope and in phase with changes in PS amplitude.
41 With these divergent effects on the fEPSP and PS, infraslow SBA ultimately modulates
42 EPSP-PS coupling and thereby enables hippocampal circuitry to generate
43 heterogeneous outputs from identical inputs. Consequently, infraslow SBA appears
44 well-suited to dynamically alter sensory selection and information processing and
45 highlights the fundamental role of endogenous neuronal activity for shaping the brain's
46 response to incoming stimuli.

47

48

49 **Significance Statement**

50 The brain's response to a given input is variable and enables flexible responses based
51 on past experience and/or current needs. Widespread, dynamic, and ever-present,
52 spontaneous brain activity may contribute to response heterogeneity by altering
53 endogenous brain states to modulate subsequent processing of exogenous information.
54 We investigated how spontaneous activity could mechanistically alter information
55 processing by assessing its role in modulating the brain's response to electrically-
56 evoked activation. We find very slow fluctuations in spontaneous activity affect evoked-
57 response variability by altering the coupling of neuronal input (i.e. depolarization) to
58 subsequent neuronal output (i.e. action potential generation). These results, therefore,
59 characterize a broad mechanism by which spontaneous brain activity can alter sensory
60 and information processing.

61

62

63

64

65

66

67

68

69

70

71

72 **Introduction**

73 Trial-to-trial responses of the brain to the same external stimuli are typically
74 heterogeneous (Fox et al., 2005; Scaglione et al., 2011). This heterogeneity could arise
75 from the stochastic nature of action potential propagation (Faisal and Laughlin, 2007)
76 and synaptic transmission (Destexhe et al., 2001; Fellous et al., 2003) leading to
77 variable neuronal activation following stimulation. Alternatively, the brain's internal
78 milieu (Fontanini and Katz, 2008), including the levels and patterns of spontaneous
79 brain activity (SBA) during stimulus presentation (Hesselmann et al., 2008), may
80 modulate its response to incoming stimuli. Characterizing how SBA affects the
81 response of the brain to incoming stimuli is critical for understanding information
82 processing and sensory selection within the brain (Sterzer et al., 2009; Jetli et al.,
83 2014).

84 SBA produces the vast majority of the brain's energetic demands, highlighting
85 the fundamental importance of task-independent activity for brain function (Raichle,
86 2011). Electrophysiological measures of SBA demonstrate that the brain produces
87 constitutive activity across wide temporal (from infraslow (<0.1Hz) to ultra-fast (upwards
88 of 600Hz)) and spatial scales (Buzsáki and Draguhn, 2004). Activity across these
89 disparate spatial and temporal scales does not occur independently, but rather, exhibits
90 complex spatiotemporal organization that in large part is coordinated by ongoing
91 infraslow activity. Spatially, distinct networks of functionally connected brain regions
92 (e.g. (Smith et al., 2009)), including the default mode network (Raichle, 2015), have
93 been identified through their correlated infraslow fluctuations in resting state fMRI
94 activity. Temporally, the phase of infraslow fluctuations in neocortical EEG activity

Infraslow SBA modulates EPSP-PS coupling

95 modulates the amplitude of activity at higher frequencies (>1Hz; (Vanhatalo et al., 2004;
96 Monto et al., 2008)). Thus, infraslow activity can exert widespread modulation of the
97 levels and patterns of SBA and consequently may regulate the brain's response to
98 incoming stimulation.

99 Perception of external stimuli can fluctuate across infraslow timescales
100 associated with ongoing fluctuations in SBA (reviewed in: (Schroeder and Lakatos,
101 2009; Sadaghiani and Kleinschmidt, 2013)). For example, conscious perception of
102 sporadic somatosensory stimulations exhibits spontaneous infraslow fluctuations that
103 are associated with both the phase of infraslow EEG fluctuations and amplitude of
104 higher frequency (1-40Hz) EEG power (Monto et al., 2008). The association between
105 performance variability and higher frequency power may indicate that infraslow SBA
106 modulates the brain's response to incoming stimuli through widespread alterations in
107 neuronal excitability. Consistent with this idea, both spontaneous interictal events
108 recorded from the cortex of epileptic patients (Vanhatalo et al., 2004) and spontaneous
109 hippocampal afterdischarges present in a subset of Wistar rats (Penttonen et al., 1999)
110 fluctuate across infraslow timescales. However, the underlying physiological
111 mechanisms responsible for infraslow changes in excitability, and for associated
112 perceptual variability, remain unclear. It has been proposed that surface recorded
113 infraslow potentials may arise as a consequence of cortico-thalamic connectivity
114 facilitating long-lasting EPSPs within neocortical dendritic processes (Birbaumer et al.,
115 1990; He and Raichle, 2009). The extent and mechanisms by which infraslow
116 fluctuations in SBA are produced outside of neocortex, and, if present, the effects of

Infraslow SBA modulates EPSP-PS coupling

117 these spontaneous fluctuations on the processing of incoming stimuli are poorly
118 characterized.

119 In the present study, we investigated the relationships between spontaneous
120 hippocampal EEG activity and trial-to-trial variability of evoked responses within the
121 dentate gyrus following electrical stimulation of the medial perforant pathway. This
122 approach allowed us to characterize the effects of SBA on both local processing of
123 incoming stimuli (field excitatory postsynaptic potential; fEPSP) and on the subsequent
124 generation of action potentials (population spike; PS). We observed infraslow
125 fluctuations in low (0.5-9Hz) and high (40-100Hz) frequency band-limited power (BLP)
126 within the hippocampus that occur anti-phase to observed infraslow fluctuations in the
127 magnitude of fEPSP slope yet occur in-phase with infraslow fluctuations in PS
128 amplitude. Thus, ongoing infraslow SBA appears to contribute to evoked response
129 variability by dynamically altering fEPSP-PS coupling of hippocampal neurons.

130

131 **Methods**

132 *Surgery*

133 3-4-month-old, male Sprague-Dawley rats (n=17, Harlan; Indianapolis IN) were housed
134 individually under standard laboratory conditions (12hr light/dark cycle, access to food
135 and water *ad libitum*). Immediately prior to surgery, rats were treated with an antibiotic
136 (penicillin; 100,000 units/kg) and NSAID analgesic (Flunixin; 2.5mg/kg). Under
137 isoflurane anesthesia (5% induction, 2.5% maintenance) electrodes were bilaterally
138 implanted as previously described (Korol and Gold, 2008) to record evoked field
139 potentials within the dentate gyrus following electrical stimulation of the medial perforant

Infraslow SBA modulates EPSP-PS coupling

140 pathway. Specifically, Teflon-coated stainless steel wires (0.003" bare diameter, A-M
141 Systems, Sequim, WA) were implanted into the hilus of the dentate gyrus (from bregma:
142 AP: -3.5 mm, ML: \pm 2 mm, DV: \sim 3.5-4 mm) and referenced to screws affixed to the skull
143 to record extracellular field potentials. Two additional Teflon-coated stainless steel
144 wires, with roughly 500 μ M of insulation removed at the end, were implanted into the
145 medial perforant pathways (AP: -8.1 mm, ML: \pm 4.2 mm, DV: \sim 3 - 3.5 mm) and
146 referenced to screws affixed to the skull to serve as stimulating electrodes. Final
147 positions for both stimulating and recording electrodes were adjusted to ensure correct
148 placement by maximizing the magnitude of the evoked potential. Recording,
149 stimulating, and screw electrodes were capped with gold Amphenol pins, placed inside
150 a 9-pin ABS plug (Ginder Scientific, Ontario, Canada), and affixed to the skull with
151 dental acrylic. Post-operative care included topical administration of antibacterial
152 ointment (Bacitracin) to the surgical site and access to analgesic for 24hrs following
153 surgery (Children's Ibuprofen; 2.35 mL in 500 mL water bottles). All rats recovered
154 undisturbed for at least 7 days following surgery before any additional experimental
155 procedures were conducted. These methods and those below were carried out in
156 accordance with the National Institutes of Health Guide for the Care and Use of
157 Laboratory Animals and were approved by the Syracuse University Institutional Animal
158 Care and Use Committee.

159

160 *Electrophysiological Recordings*

161 Evoked field potentials following electrical stimulation of the medial perforant
162 pathway were recorded from each rat in its home cage. All electrode leads were

Infraslow SBA modulates EPSP-PS coupling

163 connected to a commutator with flexible wiring to enable unobstructed movement
164 throughout the home cage. The timing of electrical stimulations was controlled by
165 computer program (Signal 4; Cambridge Electronic Design, Cambridge England) and an
166 attached microcontroller (Micro1401; Cambridge Electronic Design). Monopolar
167 stimulations (square pulses, 200 μ S duration, typically between 0.1 mA-1 mA) were
168 produced by battery-operated stimulus isolator units (World Precision Instruments A365,
169 Sarasota FL) and delivered to the stimulating electrodes. Evoked field potentials and
170 spontaneous electroencephalographic activity (EEG) were amplified (200X) and filtered
171 (high-pass: 0.3 Hz; low-pass: 3 kHz) with ac-amplifiers (Grass Technologies Model
172 P5111K, Warwick RI) and the resultant signal recorded by the computer (sampling
173 frequency = 10,000 Hz).

174 On the first day of recording for each rat, the baseline stimulation intensity was
175 determined. First, a range of stimulations was given to find the minimum stimulation
176 intensity to produce a fEPSP and to find the intensity at which no further increases in
177 fEPSP could be elicited (maximum intensity). An input/output curve of 10 stimulation
178 intensities evenly interspersed between the minimum and maximum intensity was then
179 established by recording three evoked responses at each stimulation intensity (20s
180 interstimulation interval). The slope of the fEPSP was quantified and in all cases
181 increased as a function of increasing input intensity. From this input/output curve, the
182 intensity of baseline stimulation was determined by selecting the stimulation intensity
183 that produced ~40% of the maximal fEPSP slope to ensure that future recordings would
184 be sensitive to either increases or decreases in fEPSP slope. Baseline recordings (30
185 stimulations delivered at 0.05Hz) were performed daily for at least 4 consecutive days to

Infraslow SBA modulates EPSP-PS coupling

186 confirm that stable evoked responses (daily fEPSP means not differing by more than \pm
187 5%) could be produced. On the day following establishment of a stable baseline, two
188 28-min recording sessions (10-15 min between each session) were performed. Herein,
189 electrical stimulations at baseline intensity were delivered throughout at 0.25Hz (N=10
190 rats). To test whether results from this population depended on stimulation frequency,
191 all experimental procedures and analyses were performed on a second group of rats
192 (N=7) that only differed in their stimulation frequency (0.10Hz). Evoked responses and
193 spontaneous EEG activity were recorded. All recordings were taken between 4 and 7
194 hours after vivarium light onset. Additionally, the behavioral state of the rat was
195 monitored and classified as either quiet waking (eyes-open, immobile), active waking
196 (exploratory behavior), behaviorally-defined sleep (eyes-closed, immobile), or grooming.

197 Of note, rats in the present study were previously part of a separate study
198 investigating mechanisms by which epinephrine modulates long-term potentiation (Dash
199 et al., unpublished observations). For the present study, the electrophysiological
200 recordings described above occurred: 1) at least 7 days following the completion of any
201 previous experiments, 2) only after the baseline evoked response was stable for 4
202 consecutive days, and 3) typically about 4 weeks after surgery.

203

204 *Experimental Design, Data Processing, and Statistical Analyses*

205 All data were analyzed off-line with custom scripts in Mathworks MATLAB
206 (Natick, MA). Additional statistics were performed with Statistica 6 (Statsoft, Tulsa OK).
207 Two parameters of the evoked response were quantified: 1) the fEPSP, produced by
208 the initial depolarization of neurons within the dentate gyrus following stimulation and 2)

Infraslow SBA modulates EPSP-PS coupling

209 the population spike (PS), produced by the collective firing of action potentials within the
210 population (McNaughton and Barnes, 1977). The fEPSP was quantified by measuring
211 the slope of the large positive deflection following cessation of the stimulation artifact.
212 fEPSP slopes were calculated within a ~0.4 - 0.5ms window following slope onset to
213 avoid potential confounding effects of population spike onset variability on fEPSP slope.
214 PS amplitude was quantified by first drawing a tangent between to the two apices of the
215 evoked response and then calculating the amplitude of a vertical line drawn between
216 the trough of the PS and this tangent line. To facilitate comparisons across rats, fEPSP
217 slope and PS amplitude were normalized within each rat to their respective mean
218 values across a recording session. fEPSP slope could be quantified for all rats while
219 PS amplitude could be calculated for 15 of 17 rats.

220 Spontaneous EEG activity was recorded throughout the two, 28-minute
221 recording sessions. EEG signals were down sampled to 200Hz and 60Hz line noise
222 was filtered with a zero-phase, Chebyshev type II bandstop filter. Manual rejection of
223 movement artifacts present in the EEG data was performed by visual inspection of EEG
224 data and their corresponding power spectra in 4-sec epochs. Epochs with large,
225 atypical voltage deflections and/or prominent power <0.5Hz (frequencies that cannot be
226 recorded with our ac-amplifiers) were classified as artifact and were not included in any
227 future analyses. Overall, less than 5% of epochs were rejected. Power spectra were
228 calculated via Welch's method (hamming window, 0.25Hz resolution) for each 4 sec
229 epoch of spontaneous EEG data. EEG BLP was calculated by averaging the total
230 power present within distinct frequency bands (delta: 0.5-4Hz; theta: 5-9Hz; alpha: 10-
231 18Hz; beta: 22-30Hz; highbeta: 30.25-40Hz; lowgamma: 40.25-59Hz; midgamma: 61-

Infraslow SBA modulates EPSP-PS coupling

232 80Hz; highgamma: 80.25-100Hz). As similar results were obtained throughout this
233 study from neighboring frequency bands, BLP for three broad frequency bands was also
234 calculated (low frequencies: 0.5-9Hz; middle frequencies: 10-40Hz; high frequencies:
235 40.25-100Hz). Time series of BLP were created across the entire recording session
236 and power spectra of these time series were obtained as above to assess whether
237 infraslow (<0.1Hz) fluctuations in BLP were present.

238 Multiple approaches were taken to quantify the relationships between
239 hippocampal evoked response variability and spontaneous brain activity. Two of these
240 approaches were conducted in the time domain. First, we calculated Pearson's
241 correlation coefficients between BLP at each frequency band in the four seconds
242 preceding each evoked response and either fEPSP slope or PS amplitude for each
243 individual rat. Second, we binned all evoked responses into quartiles as a function of
244 the amount of BLP in the preceding four seconds. The average fEPSP slope and PS
245 amplitude were calculated within each quartile and the significance of these results was
246 assessed with a repeated measures ANOVA.

247 Additional analyses were conducted in the frequency domain. Missing data
248 points in BLP time series (due to previous artifact rejection) were linearly interpolated to
249 enable digital filtering. Time series of BLP, fEPSP slope, and PS amplitude across each
250 recording session were filtered in the infraslow range with a zero-phase, type II
251 Chebyshev filter (band pass: 0.004-0.025Hz). For each signal, we calculated the angle
252 of the complex vector obtained from the Hilbert transform to provide a measure of
253 instantaneous phase (Vanhatalo et al., 2004). Instantaneous phase differences (IPD)
254 were calculated as follows: $IPD = e^{i*(P_1 - P_2)}$ wherein P_1 and P_2 are the instantaneous

Infraslow SBA modulates EPSP-PS coupling

255 phase of the two signals being compared. The average of IPD is a complex number in
256 which the imaginary component is the average phase difference and the real part is the
257 phase locking factor (PLF). The PLF ranges from 0-1 with values near 0 representing a
258 uniform phase distribution and values near 1 indicating perfect phase synchrony
259 (Vanhatalo et al., 2004). To assess the significance of the obtained IPD and PLF,
260 distributions of random IPDs and PLFs were created by repeating the same analyses
261 described above 1000 times for each rat with randomized fEPSP and PS data. Overall,
262 actual IPDs and PLFs were compared to the randomized data to determine if the
263 relationships observed in the actual data reflect true phase locking or rather, arise
264 simply due to chance.

265 We used a complementary method to address further the relationship between
266 infraslow BLP activity and evoked response magnitude. Herein, evoked responses were
267 binned as a function of the instantaneous phase of infraslow BLP. fEPSP slope and PS
268 amplitude were averaged within each bin. Lastly, the ratio of fEPSP slope and PS
269 amplitude was calculated as a measure of fEPSP-PS coupling. fEPSP-PS coupling
270 reflects the amount of output produced (PS) by a given input (fEPSP; (Daoudal and
271 Debanne, 2003; Zsiros and Hestrin, 2005)). To investigate how ongoing spontaneous
272 brain activity affects fEPSP-PS coupling, we binned and averaged this fEPSP-PS ratio
273 as a function of infraslow BLP phase.

274 Throughout this study, all results are expressed as the arithmetic mean \pm SEM
275 with the exception of phase differences which are expressed as the circular mean \pm
276 circular standard deviation (Berens, 2009). Circular means are presented as positive
277 angles along the unit circle between 0 and 2π .

278 **Results**279 *Extensive variability of evoked response and spontaneous EEG activity*

280 The slope of the evoked field excitatory post-synaptic potential (fEPSP) and
281 amplitude of population spike (PS) can be used to quantify the response of a neuronal
282 population to incoming stimulation. Increased stimulation intensity typically results in an
283 increased fEPSP slope and elevated PS amplitude. Notably, evoked response
284 magnitude can vary considerably even when stimulation intensity is held constant.
285 During 28-minute recording sessions (see methods and Figure 1 for experimental
286 design), we recorded 420 evoked responses in the dentate gyrus following stimulation
287 of the perforant pathway (0.25Hz; n=10). Extensive trial-to-trial variability of the fEPSP
288 slope and PS amplitude was observed (Figure 1), with a large average standard
289 deviation of the fEPSP ($11.66 \pm 2.10\%$ mean fEPSP) and PS ($37.93 \pm 5.00\%$ mean PS)
290 across all animals. We also observed extensive evoked response variability when rats
291 were stimulated at 0.10Hz (n=7) including large average standard deviations of the
292 fEPSP ($14.69 \pm 2.37\%$ mean fEPSP), PS ($22.11 \pm 3.51\%$ mean PS). To assess
293 whether spontaneous brain activity exhibits similar variability to the evoked responses,
294 we calculated the amount of broadband EEG power (0.5-100Hz) in four seconds
295 epochs preceding each evoked response. Four second epochs of broadband EEG
296 power also exhibited substantial variability (Figure 1; average standard deviation: 41.43
297 $\pm 3.56\%$ mean total power) raising the possibility that changes in spontaneous brain
298 activity are associated with the observed evoked response variability.

299 fEPSP slope and PS amplitude variability do not appear to arise primarily as
300 consequences of systemic changes in perforant path – dentate gyrus connectivity

Infraslow SBA modulates EPSP-PS coupling

301 resulting from prolonged stimulation. While fEPSP slopes and PS amplitudes recorded
302 from rats stimulated at 0.25Hz were on average smaller in the second half of recordings
303 ($97.35 \pm 1.25\%$, $t(19) = -2.13$, $p=0.047$ and $87.45 \pm 3.53\%$, $t(17) = -3.55$, $p=0.0025$,
304 respectively) than in the first half of recordings, linear regression reveals that time of
305 stimulation only account for 3.3% of the total variance in fEPSP slope and 13.2% of total
306 PS amplitude variance. Moreover, first and second half fEPSP slopes were not
307 significantly different ($t(13) = -0.68$, $p=0.51$) in 0.10Hz stimulated rats with time of
308 stimulation only accounting for 1.1% of total fEPSP variance in this population.
309 Likewise, PS amplitudes in 0.10Hz stimulated rats were not significantly affected by
310 time of stimulation ($t(11) = -0.79$, $p=0.44$, with time of stimulation accounting for only
311 2.1% of total PS amplitude variation).

312

313 *Antecedent EEG activity is associated with evoked response variability*

314 We calculated the correlations between BLP in the four seconds preceding each
315 evoked response and the ensuing fEPSP or PS. Similar patterns of correlation were
316 observed across all rats regardless of stimulation frequency wherein the strength of
317 correlation varied as a consequence of BLP frequency and the component of the
318 evoked response (Figure 2). Specifically, negative correlations were typically observed
319 between the fEPSP slope and both low-frequency BLP (0.5-9Hz; average correlation:
320 $r_{0.25} = -0.31 \pm 0.02$, $r_{0.10} = -0.38 \pm 0.09$,) and high frequency BLP (40.25-100Hz; $r_{0.25} = -$
321 0.38 ± 0.03 , $r_{0.10} = -0.42 \pm 0.11$). By contrast, correlations between fEPSP slope and
322 middle frequency BLP (10-40Hz) were heterogeneous across individual rats and on
323 average small ($r_{0.25} = -0.05 \pm 0.04$, $r_{0.10} = -0.17 \pm 0.11$). A similar frequency

Infraslow SBA modulates EPSP-PS coupling

324 dependence was observed between BLP and the PS amplitude. PS amplitude,
325 however, was positively correlated with preceding low frequency BLP ($r_{0.25} = 0.26 \pm$
326 0.04 , $r_{0.10} = 0.27 \pm 0.13$) and high frequency BLP ($r_{0.25} = 0.26 \pm 0.05$, $r_{0.10} = 0.28 \pm 0.11$).
327 Again, these correlations were not evident when comparing PS amplitude and middle
328 frequency BLP ($r_{0.25} = 0.02 \pm 0.04$, $r_{0.10} = -0.03 \pm 0.09$). Thus, preceding spontaneous
329 brain activity in the low and high frequencies was negatively correlated with fEPSP
330 slope and positively correlated with PS amplitude.

331 To quantify the relationships between BLP and evoked response magnitude
332 further, all 4-second epochs of spontaneous activity were subdivided into BLP quartiles
333 and the average fEPSP slope or PS amplitude was calculated within each quartile
334 (Figure 3). Consistent with the correlations above, fEPSP slope and PS amplitude
335 varied in association with amount of BLP in the low and high, but not middle,
336 frequencies. Evoked responses following epochs that contained the least low frequency
337 power had larger fEPSP slopes and smaller PS amplitude than responses following
338 epochs that contained the most power (see Figure 3 for example evoked responses). A
339 similar trend was observed across high frequency BLP quartiles, but was absent across
340 middle frequency BLP quartiles. Overall, when characterizing fEPSP variability, a
341 significant main effect of BLP quartile ($F(3,45) = 16.94$, $p = 1.66 \times 10^{-7}$) and a significant
342 interaction between BLP quartile and BLP frequency ($F(6,90) = 7.61$, $p = 1.28 \times 10^{-6}$)
343 were observed. These effects appear to be independent of stimulation frequency as we
344 did not observe significant interactions between stimulation frequency and either BLP
345 quartile or the three-way interaction of quartile, BLP frequency, and stimulation
346 frequency ($F(3,45) = 0.84$, $p = 0.48$, and $F(6,90) = 0.81$, $p = 0.56$). When characterizing PS

Infraslow SBA modulates EPSP-PS coupling

347 variability, a significant main effect of BLP quartile ($F(3,39) = 12.56, p=6.86 \times 10^{-6}$) and
348 a significant interaction between BLP quartile and BLP frequency ($F(6,78)=5.65, p=6.51$
349 $\times 10^{-5}$) was also observed. Again, stimulation frequency did not appear to alter these
350 effects (interaction, stimulation frequency by BLP quartile: $F(3,39) = 0.20, p=0.90$;
351 interaction, stimulation frequency by BLP quartile by BLP frequency: $F(6,78) = 1.21,$
352 $p=0.31$)

353

354 *Infraslow fluctuations in EEG activity are associated with evoked response variability*

355 The above analyses solely focus on the relationships between evoked responses
356 and the preceding 4-sec epochs of EEG BLP and as such are unable to determine the
357 source(s) of the variability of BLP and/or the evoked responses. Previous reports
358 indicate that neocortical BLP exhibits infraslow ($< 0.1\text{Hz}$) fluctuations in total power that
359 are associated with changes in neuronal excitability (Vanhatalo et al., 2004). To
360 investigate whether the observed variability in BLP and evoked response were, in part,
361 driven by fluctuations on a similar timescale, we created time-series of EEG BLP,
362 fEPSP slope, and PS amplitude across each recording session. Figure 4 depicts the
363 power spectra of the time-series of EEG BLP for low, middle, and high frequencies.
364 Across infraslow frequencies (0.005 - 0.02Hz) we observed broad peaks in the power
365 spectra for low and high frequency BLP that were absent in the BLP of middle
366 frequencies. Consequently, we filtered the EEG BLP time series in the infraslow range.
367 Consistent with the broad infraslow peaks present in the power spectra,
368 autocorrelograms of infraslow-filtered low and high frequency BLP (Figure 4), which lack
369 discrete peaks of high correlation except those surrounding zero lag, further

Infraslow SBA modulates EPSP-PS coupling

370 demonstrate that this infraslow activity is best characterized as a non-harmonic
371 fluctuation rather than a continuous harmonic oscillation. Specifically, cycle-to-cycle
372 variation in period length occurred throughout our recording sessions, with average
373 period lengths of 1.56 ± 0.07 and 1.37 ± 0.07 min, for infraslow-filtered low and high
374 frequency BLP, respectively. Additionally, while these non-harmonic fluctuations were
375 continuously present throughout all recording periods, the peak-to-trough amplitude of
376 each cycle also varied considerably: The average standard deviation of within-session
377 peak-to-trough amplitudes for high frequency BLP was $38.79 \pm 12.87\%$ and for low
378 frequency BLP was $60.50 \pm 21.42\%$ of mean peak-to-trough amplitude. Thus it appears
379 as though very slow, non-harmonic fluctuations in spontaneous brain activity are
380 present in low and high frequency BLP and, moreover, that the period length and
381 amplitude of these fluctuations can vary across time.

382 Infraslow EEG BLP may be associated with the observed fEPSP slope and PS
383 amplitude variability. To assess this possibility, we filtered fEPSP slope and PS
384 amplitude time series in the infraslow range and calculated instantaneous phase
385 differences between each of these measures (see Figure 4 for example data from an
386 individual rat). To quantify these phase differences across all rats, we calculated the
387 distribution of phase differences between BLP and either fEPSP slope or PS amplitude
388 for our observed data and compared these distributions to random distributions
389 obtained by comparing phase differences of our shuffled data. As seen in Figure 5,
390 infraslow fluctuations in fEPSP slope were typically antiphase to infraslow fluctuations in
391 low-frequency BLP (circular phase difference mean (PD) in radians \pm circular standard
392 deviation: $PD_{0.25} = 3.34 \pm 0.63$, $PD_{0.10} = 2.80 \pm 1.10$) and high-frequency BLP ($PD_{0.25} =$

Infraslow SBA modulates EPSP-PS coupling

393 3.25 ± 0.32 , $PD_{0.10} = 3.00 \pm 0.95$). To assess the significance of these phase
394 differences, we calculated the phase locking factor (PLF) for the observed data and
395 compared these values to PLFs calculated from shuffled data. Significant phase-
396 locking (i.e. experimentally observed PLFs greater than 95% of all PLFs obtained from
397 1000 iterations of shuffled data) between fEPSP slope and both low-frequency BLP
398 ($PLF_{0.25} = 0.40$; $p < 0.01$, $PLF_{0.10} = 0.29$; $p < 0.05$) and high-frequency BLP ($PLF_{0.25} =$
399 0.40 ; $p < 0.01$, $PLF_{0.10} = 0.28$; $p < 0.05$) was observed. In contrast, significant phase
400 locking was absent between infraslow fluctuations of fEPSP slope and middle-frequency
401 BLP ($PLF_{0.25} = 0.18$; $p > 0.05$, $PLF_{0.10} = 0.13$; $p > 0.05$). The relationship between PS
402 amplitude and spontaneous BLP exhibited a similar frequency dependency to the
403 relationship between fEPSP slope and BLP (Figure 5). However, infraslow fluctuations
404 in PS amplitude and low and high frequency BLP were in phase ($PD_{0.25}$: 0.79 ± 1.58 ;
405 0.50 ± 0.83 , respectively, $PD_{0.10}$: 6.01 ± 1.07 ; 6.02 ± 1.30 , respectively). Again, this
406 phase locking was significant, or trended significant, for low ($PLF_{0.25} = 0.26$, $p < 0.05$,
407 $PLF_{0.10} = 0.30$ $p < 0.05$) and high ($PLF_{0.25} = 0.27$, $p < 0.05$, $PLF_{0.10} = 0.21$ $0.05 < p < 0.10$)
408 frequency BLP, but not statistically significant for middle frequency BLP ($PLF_{0.25} = 0.13$
409 $p > 0.05$, $PLF_{0.10} = 0.18$ $p > 0.05$).

410 To quantify the effects of the ongoing phase of infraslow brain activity on evoked
411 response magnitude, fEPSP slope and PS amplitude for each evoked response were
412 binned and averaged as a function of ongoing infraslow BLP phase (Figure 6). A
413 significant main effect of infraslow phase ($F(7, 105) = 16.87$, $p = 9.10 \times 10^{-15}$) and a
414 significant interaction between phase and BLP frequency ($F(14, 210) = 4.08$, $p = 2.90 \times$
415 10^{-6}) was found to affect fEPSP slope. No significant interactions between stimulation

Infraslow SBA modulates EPSP-PS coupling

416 frequency and infraslow phase ($F(7,105) = 0.32, p=0.95$) or between stimulation
417 frequency, infraslow phase, and BLP frequency ($F(14,210) = 1.12, p=0.34$) were
418 observed to affect fEPSP slope. Infraslow phase significantly affected PS amplitude (F
419 $(7,91) = 4.39, p=3.09 \times 10^{-4}$) and a significant interaction between phase and BLP
420 frequency ($F(14,182) = 2.42, p=0.004$) was found to affect PS amplitude. No significant
421 interactions between stimulation frequency and infraslow phase ($F(7,91) = 1.56,$
422 $p=0.15$) or between stimulation frequency, infraslow phase, and BLP frequency (F
423 $(14,182) = 0.94, p=0.52$) were observed to affect PS amplitude. Overall fEPSP slope
424 was steepest and PS amplitude the smallest during nadirs of the infraslow fluctuation in
425 either low or high frequency BLP. The instantaneous phase of middle frequency BLP
426 did not appear to affect either the fEPSP slope or PS amplitude. Thus, spontaneous
427 infraslow fluctuations in low and high frequency BLP are associated with evoked
428 response variability and appear independent of stimulation frequency.

429 The opposing effects of infraslow BLP fluctuations on the fEPSP and PS indicate
430 that coupling of incoming depolarization (fEPSP) with output (PS) varies dynamically in
431 the dentate gyrus as a function of ongoing spontaneous brain activity. As evident in
432 Figure 6, EPSP-PS coupling changed in association with changing phase of infraslow
433 fluctuations in low/high frequency BLP but showed no association with fluctuating BLP
434 in the middle frequencies. Specifically, the phase of infraslow BLP significantly affected
435 the degree of EPSP-PS coupling ($F(7,91) = 13.96, p=3.62 \times 10^{-12}$) and moreover, the
436 effect of phase was modulated by the frequency of BLP ($F(14,182) = 6.95, p=2.38 \times$
437 10^{-11}). No significant effects of stimulation frequency were observed (interaction
438 between stimulation frequency and infraslow phase: $F(7,91) = 0.49, p=0.84$, interaction

Infraslow SBA modulates EPSP-PS coupling

439 between stimulation frequency, infraslow phase, and BLP quartile: $F(14,182) = 0.81$,
440 $p=0.66$). Thus, independent of stimulation frequency, EPSP-PS coupling is maximal at
441 the peak of infraslow fluctuations in low or high frequency BLP (~10-15% higher than
442 average) and minimal during the nadir of infraslow fluctuations in low or high frequency
443 BLP (~10-15% lower than average).

444

445 *Changes in behavioral state do not appear responsible for infraslow EEG*
446 *fluctuations and associated evoked response variability*

447 Hippocampal evoked response magnitude varies in association with behavioral
448 state (Coenen, 1975; Winson and Abzug, 1977; Green et al., 1990). To determine
449 whether infraslow variability observed in the present study is a reflection of behavioral
450 state fluctuations, we assessed the relationships between behavior, evoked response
451 magnitude, and infraslow activity. Behavioral data were only recorded for rats
452 stimulated at 0.25Hz and thus all behavioral data presented are from this group only.
453 Throughout the recording sessions, rats exhibited quiet wakefulness for the majority of
454 time observed ($66.33 \pm 10.08\%$) with the remainder of time filled with exploratory
455 waking ($23.00 \pm 9.21\%$), behaviorally-defined sleep ($8.00 \pm 8.99\%$) and active grooming
456 ($2.67 \pm 3.67\%$). Similar to previous reports (Green et al., 1990; Moser et al., 1993),
457 fEPSP slopes evoked during periods of active waking were significantly steeper than
458 those evoked during quiet waking (active fEPSP slope $107.87 \pm 2.92\%$ of quiet waking;
459 $t(9) = 2.70$, $p=0.024$), while PS amplitudes trended lower (active PS amplitude $79.33 \pm$
460 8.77% of quiet waking; $t(8) = 2.04$, $p=0.076$).

Infraslow SBA modulates EPSP-PS coupling

461 This state-dependent variability, however, does not appear well-suited to explain
462 infraslow variability in evoked response magnitude discussed above. Infraslow
463 fluctuations in evoked response magnitude were observed across all rats, yet rats
464 varied considerably in the amount of time spent in each behavioral state (e.g. time spent
465 in quiet waking ranged from 43.33% to 96.67% of total recording time). Moreover, the
466 average bout duration for quiet waking (11.96 ± 2.71 min) and active waking ($4.47 \pm$
467 0.82 min) were both considerably longer than the average period of infraslow
468 fluctuations in fEPSP slope (1.37 ± 0.04 min) or PS amplitude (1.27 ± 0.03 min).
469 Multiple infraslow cycles, therefore, can occur without alternation of behavioral state.

470 To assess this possibility directly and to determine if the infraslow oscillations in
471 fEPSP slope or PS amplitude described above were related to behavioral state
472 dependent changes in evoked response magnitude, we examined whether the
473 distribution of instantaneous infraslow phases deviated from a uniform distribution
474 during periods of quiet or active waking. If behavioral state were biasing the infraslow
475 phase distribution, we would expect to see a non-uniform phase distribution within each
476 behavioral state. Conversely, a uniform distribution indicates that complete cycles of
477 infraslow oscillations readily occur without changes in behavioral state and therefore it is
478 unlikely that the infraslow oscillations are driven by behavioral state. For both fEPSP
479 slope and PS magnitude, we did not observe significant deviations from a uniform
480 distribution in either active waking (Rayleigh_z = 1.42, p = 0.243) or quiet waking
481 (Rayleigh_z = 1.73, p=0.178). Thus, we did not find evidence to support that the
482 infraslow fluctuations in evoked response magnitude described herein are byproducts of
483 behavioral state changes. Moreover, behavioral state did not appear to affect infraslow

Infraslow SBA modulates EPSP-PS coupling

484 fluctuations of low or high frequency BLP as average infraslow cycle durations (low: $t(9)$
485 = 1.15, $p = 0.28$; high: $t(9) = 0.44$, $p=0.67$) and mean peak-to-trough amplitudes (low:
486 $t(9) = 0.59$, $p = 0.57$; high: $t(9) = 0.71$, $p=0.50$) did not significantly differ between active
487 and quiet waking.

488

489 **Discussion**

490 We observed extensive variability of electrically evoked responses within the
491 hippocampus that were independent of stimulation frequency (0.1 or 0.25Hz). The
492 responses were associated with antecedent levels of both low and high frequency BLP.
493 Throughout our recording periods, low and high frequency BLP exhibited spontaneous
494 infraslow fluctuations (< 0.1 Hz) that contributed to the observed trial-to-trial variability of
495 the evoked response by dynamically altering the generation of action potentials in
496 response to postsynaptic depolarization (fEPSP-PS coupling). Together these results
497 provide evidence that 1) the hippocampus exhibits infraslow fluctuations in SBA with a
498 periodicity similar to those previously described in neocortex and 2) the effects of
499 infraslow SBA on the processing of incoming stimuli may arise as a consequence of
500 changes in fEPSP-PS coupling.

501 Infraslow fluctuations in spontaneous BOLD fMRI signals (Smith et al., 2009;
502 Raichle, 2015), full band EEG (Vanhatalo et al., 2004), and BLP of higher frequencies
503 (>0.1 Hz; (Monto et al., 2008) have been reported throughout neocortex. Our
504 observation of slow (0.004 – 0.025Hz), non-harmonic oscillatory activity with extensive
505 variation in cycle-to-cycle peak-to-trough amplitudes provides novel empirical support
506 establishing the presence of similar spontaneous infraslow activity within hippocampal

Infraslow SBA modulates EPSP-PS coupling

507 networks. Notably however, this hippocampal infraslow activity is associated with a
508 distinct pattern of modulation of BLP of higher frequencies with fluctuations in low (0.5 -
509 9Hz) and high (40.25 - 100Hz) frequency BLP that were largely absent in middle
510 frequency BLP (10 - 40Hz).

511 The coordinated activity of low and high frequency hippocampal activity may, in
512 part, arise from extensive theta-gamma coupling characteristic of hippocampal
513 ensembles (Jensen and Colgin, 2007; Shirvalkar et al., 2010). Prominent theta activity
514 within the hippocampus occurs as a consequence of its distinct cellular composition
515 (replete with a diversity of morphologically and functionally distinct inhibitory
516 interneurons; (Freund and Buzsaki, 1996), and connectivity (e.g. medial septal
517 cholinergic input; (Mitchell et al., 1982)). Coordination of rhythmic pyramidal cell
518 excitation across the theta cycle with inhibitory signaling couples ongoing theta activity
519 to the generation of gamma oscillations (Wulff et al., 2009; Colgin, 2015). These
520 intrinsic hippocampal characteristics may therefore account for the frequency-
521 dependent associations of our observed infraslow SBA; this observation is consistent
522 with the region-dependent coupling of high-frequency BLP and infraslow activity first
523 identified within functionally distinct resting state fMRI networks (Mantini et al., 2007).
524 Infraslow SBA, therefore, is present across many brain regions although its effects on
525 the power of higher frequency oscillatory activities appear to be constrained by region-
526 specific functional connectivity and/or cellular phenotype.

527 Despite the ubiquity of infraslow activity throughout the brain, the physiological
528 mechanisms responsible for infraslow SBA are not well characterized. Regionally
529 heterogeneous infraslow activity could result from 1) stochastic resonance leading to

Infraslow SBA modulates EPSP-PS coupling

530 the formation of dynamic assemblies and/or 2) intrinsic oscillatory activity present within
531 neuronal or astrocytic cells at infraslow timescales (Deco and Corbetta, 2011; Palva and
532 Palva, 2012; Zylbertal et al., 2017). Biochemically, infraslow activity has been
533 associated with activation of adenosine A1 receptors (Lőrincz et al., 2009; Lindquist and
534 Shuttleworth, 2012), regenerative calcium waves within networks of astrocytes (Kuga et
535 al., 2011), and activity of subcortical neuromodulatory centers including the locus
536 coeruleus and raphe nucleus (Filippov et al., 2004). These physiological signals may
537 ultimately modulate neuronal excitability across infraslow timescales through the
538 emergence of spontaneous fluctuations in resting membrane potential
539 (Chan et al., 2015).

540 The observed changes in fEPSP-PS coupling that were contingent upon the
541 phase of infraslow SBA could arise as a direct consequence of these membrane
542 potential fluctuations. fEPSP-PS coupling has previously been shown to vary along with
543 intrinsic changes in postsynaptic excitability (Daoudal and Debanne, 2003; Zsiros and
544 Hestrin, 2005), and moreover is regulated by many of the same neuromodulatory
545 systems detailed above. Specifically, adenosine (Ferguson and Stone, 2010),
546 norepinephrine (Kitchigina et al., 1997), and serotonin (Klanchnik and Phillips, 1991)
547 have all been shown to alter fEPSP-PS coupling within the dentate gyrus. Moreover,
548 changes in granule cell excitability have been previously proposed (Bramham, 1998) to
549 explain a similar decoupling of fEPSP and PS amplitude to that observed in the present
550 study. During spontaneous dentate spikes, transient hippocampal phenomena that are
551 associated with the depolarization of granule cells (Penttonen et al., 1997), Bramham
552 (1998) observed decreases in fEPSP slope that were nevertheless associated with

Infraslow SBA modulates EPSP-PS coupling

553 increased PS amplitude. Thus, when granule cells within the dentate gyrus are
554 relatively hyperpolarized, electrostatic driving forces, potentially augmented by
555 facilitating effects of enhanced ephaptic coupling (Berretta et al., 2000), may produce
556 enhanced fEPSPs that nevertheless fail to reach the threshold for action potential
557 generation. By contrast, even minimal additional postsynaptic depolarization in a
558 depolarized neuron may generate spiking activity.

559 Changes in fEPSP-PS coupling of granular neurons could produce widespread
560 alterations in hippocampal spiking activity and consequent information processing.
561 Dentate granule cell firing (i.e. PS) filters entorhinal inputs (i.e. EPSPs), effectively
562 selecting what information can be processed within hippocampal circuitry (Hsu, 2007).
563 The dendritic morphology of granule cells is well-suited to yield a narrow time window
564 during which temporal summation of EPSPs may generate an action potential (Schmidt-
565 Hieber et al., 2007). Precise control of fEPSP-PS coupling is critical for subsequent
566 mossy fiber-CA3 signaling, with high rates of granule cell discharge required to reliably
567 activate CA3 pyramidal neurons (Henze et al., 2002). Ultimately, the precise control of
568 the level and timing of granule cell output contributes to hippocampal function including
569 pattern separation (Leutgeb et al., 2007), spatial navigation (Jung and McNaughton,
570 1993), and memory formation (Lisman, 1999). The observed changes in fEPSP-PS
571 coupling across infraslow timescales in the present study, therefore, could function to
572 modulate information transfer from entorhinal inputs to hippocampal circuitry.
573 Specifically, infraslow phases associated with weak fEPSP-PS coupling would enable
574 granule cells to act as a stringent, yet highly specific, filter, with only large coincident

Infraslow SBA modulates EPSP-PS coupling

575 entorhinal inputs sufficient to generate the high rates of granule firing required to reliably
576 activate downstream CA3 targets (Henze et al., 2002).

577 Dynamic fEPSP-PS coupling across infraslow scales could likewise underlie
578 previous observations of infraslow SBA modulating information processing and sensory
579 selection (Fontanini and Katz, 2008; Schroeder and Lakatos, 2009; Sadaghiani and
580 Kleinschmidt, 2013). Variations in the neuronal input/output function could account for
581 prominent variability in stimulus detection across infraslow timescales (Monto et al.,
582 2008), and is consistent with previous observations in which SBA led to the formation of
583 distinct neuronal ensembles that incorporate information about both endogenous and
584 exogenous activity (Jones et al., 2007). Endogenous infraslow activity may be subject
585 to modulation itself, thereby providing an active mechanism to tune the response of the
586 brain to incoming stimuli. For example, the amount of resting-state competition at
587 infraslow timescales between task-positive and task-negative brain networks is
588 correlated with individual performance on the Eriksen flanker task (Kelly et al., 2008).
589 Infraslow activity at rest can additionally be modulated by attention (Broyd et al., 2011)
590 or previous experience (Lewis et al., 2009) to further alter information processing within
591 distinct networks. Thus, infraslow SBA, and by extension here, fEPSP-PS coupling,
592 may be subject to both top-down and bottom-up modulation and consequently are well-
593 suited to dynamically alter the brain's response to incoming stimuli. Notably, in both the
594 present study and in previous characterizations of infraslow activity (reviewed in Palva
595 and Palva, 2012), the cycle duration and amplitude of each infraslow fluctuation
596 appears to be highly variable. Such variability may reflect the dynamic regulation of
597 infraslow activity and by extension, the dynamic modulation of fEPSP-PS coupling and

Infraslow SBA modulates EPSP-PS coupling

598 information processing. With its well-characterized morphology, circuitry, evoked
599 responses, and our present characterization of infraslow-mediated alterations in fEPSP-
600 PS coupling, the dentate gyrus presents an ideal milieu for further exploration of the
601 dynamic modulation of infraslow activity and resultant effects on brain function.

602 Behavioral state and higher frequency EEG activity have previously been
603 reported to affect trial-to-trial variability of dentate responses. Dentate evoked
604 responses during slow-wave sleep exhibit smaller EPSPs along with larger and earlier
605 PS's as compared to inactive waking (Winson and Abzug, 1977; Bramham and Srebro,
606 1989). Evoked responses are further subject to modulation within the same behavioral
607 state. During periods of active exploration, hippocampal evoked responses recorded
608 from rats have larger EPSPs and decreased PS area (Green et al., 1990). Such
609 changes may be subject to modulation by the environment being explored as evoked
610 responses recorded after rats find a novel object on the hole-board maze have larger
611 PS amplitudes than those recorded from following exploration of empty holes (Kitchigina
612 et al., 1997). Active exploration is typically associated with increased hippocampal
613 theta power (Coenen, 1975; Green et al., 1990), which may mediate some of the
614 evoked response variability. For example, EPSP slope is larger during periods in which
615 the EEG from anesthetized rats was dominated by the slow-oscillation (0.5-1.5Hz) as
616 compared to those dominated by theta (3-4Hz). Moreover, as in the present study, the
617 phase of ongoing oscillatory activity has been associated with evoked response
618 variability; stimulations delivered on the falling phase of either the slow or theta
619 oscillation produced significantly larger EPSPs than those delivered during the rising
620 phase (Schall et al., 2008). Strikingly, such variability may have important

Infraslow SBA modulates EPSP-PS coupling

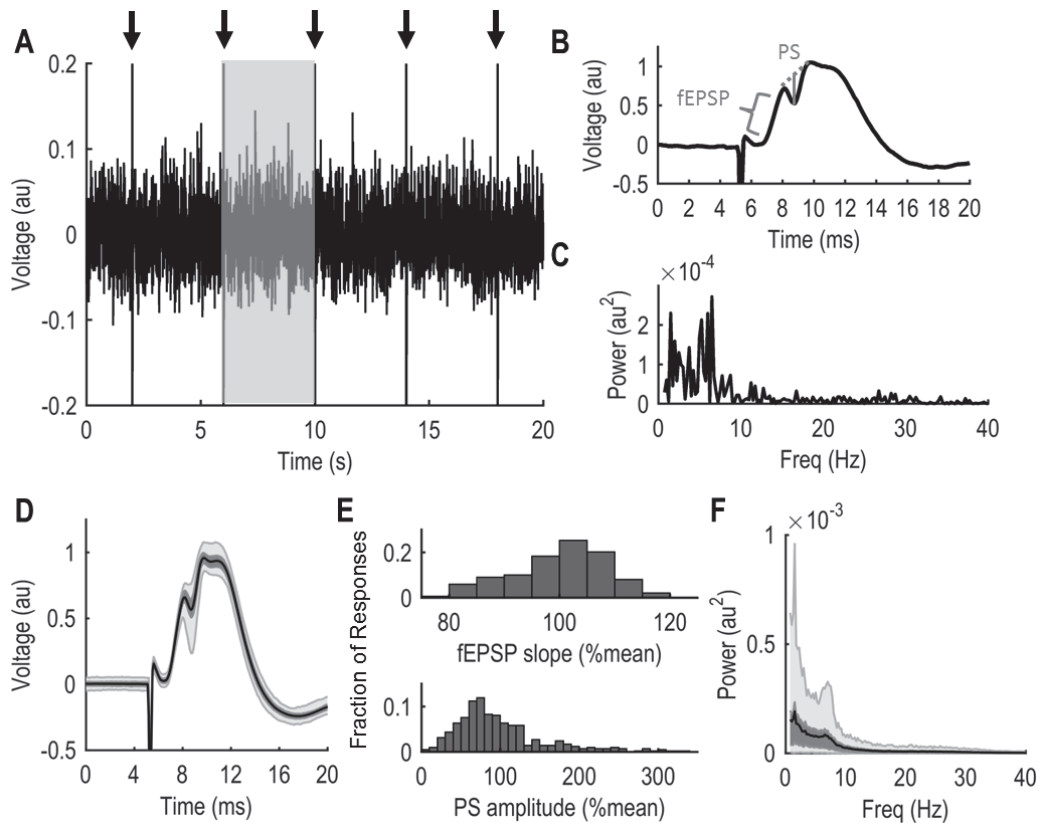
621 consequences for hippocampal function. High frequency stimulation delivered at the
622 peak of theta oscillations resulted in long-term potentiation while similar stimulation
623 delivered at the trough resulted in long-term depression (Hyman et al., 2003). With
624 similar effects on evoked response magnitude, infraslow SBA observed in the present
625 study may complement the mechanisms described above and likewise modulate
626 hippocampal function. Infraslow modulation, however, appears to be a distinct
627 phenomenon that is not directly related to behavioral state-dependent modulations (see
628 Results).

629 It has been noted that SBA is responsible for the majority of the brain's energetic
630 demands (Raichle, 2011). The relative abundance of intrinsic activity aligns well with
631 anatomically connectivity wherein the vast majority of synapses do not receive direct
632 sensory input. This predominance of endogenous brain activity exemplifies its
633 important role in regulating brain function. Our observation that spontaneous, infraslow
634 fluctuations are associated with alterations in fEPSP-PS coupling provides a putative
635 mechanism by which sensory selection and information processing can be regulated by
636 ongoing SBA. By modulating these critical functions, infraslow SBA can contribute to
637 behavioral and cognitive flexibility, and, with its potential to coordinate brain activity
638 across diverse temporal and spatial scales, may even contribute to the emergence of
639 consciousness itself (He and Raichle, 2009).

640

641

Infraslow SBA modulates EPSP-PS coupling

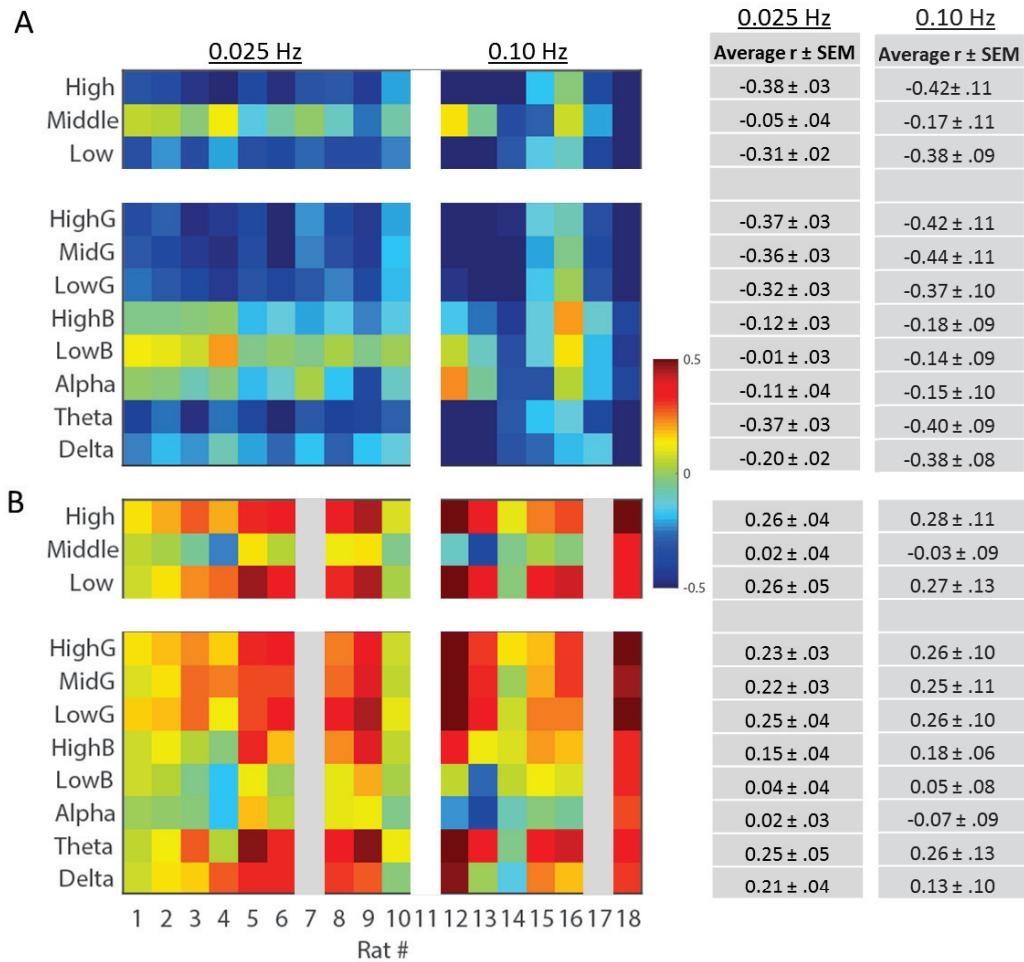


642

643 Figure 1. Extensive variability of evoked response magnitude and spontaneous EEG
 644 power during a 28-min continuous recording session. A) 20s of raw EEG data from an
 645 individual rat. Arrows denote electrical stimulation to produce an evoked response. B) A
 646 typical evoked response. To quantify the evoked response, fEPSP slope is calculated
 647 within the bracketed region while PS amplitude (solid grey line) is the amplitude from
 648 response trough to the tangent line connecting response peaks (dotted line). C) Power
 649 spectrum of spontaneous EEG activity from the 4s shaded region in A). D) Average
 650 evoked response from all 420 stimulations during a recording session in a single rat. E)
 651 Extensive variability in the evoked response is observed in both the fEPSP slope (top)
 652 and PS amplitude (bottom). F) The power spectrum of spontaneous brain activity
 653 averaged across all 4s epochs of the recording session. Power spectra were calculated
 654 from 0.5-100Hz but are only depicted to 40Hz here for enhanced visualization. In
 655 panels D and F, dark shaded regions encompass the middle 50% of all observed values
 656 and light shaded regions encompass 95% of all observed values. Similar variability in
 657 both evoked responses magnitude and EEG power was observed when the stimulation
 658 frequency was 0.10Hz instead of 0.25Hz (see results).

659

Infraslow SBA modulates EPSP-PS coupling



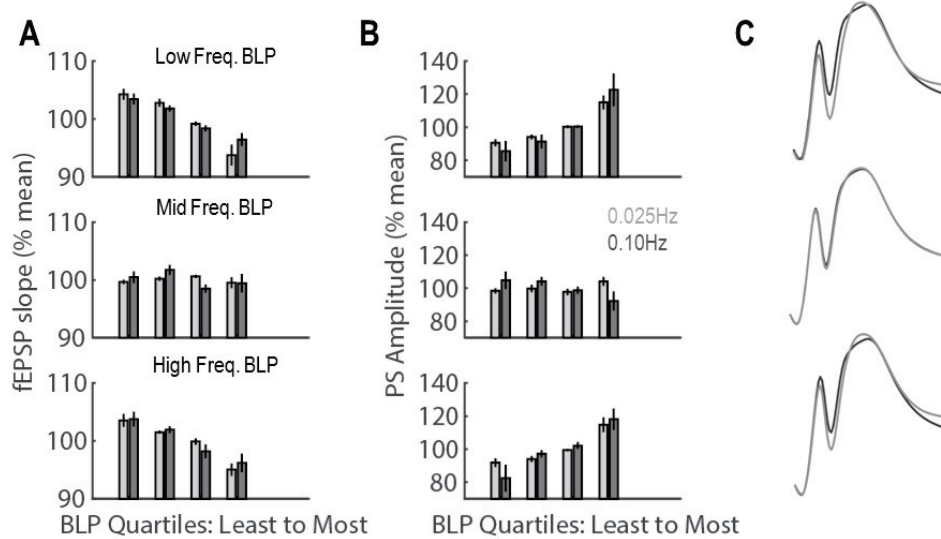
660

661 Figure 2. Correlations between antecedent EEG power and fEPSP slope (A) or PS
 662 amplitude (B) at stimulation frequencies of either 0.25 or 0.10Hz. Heat maps depict
 663 correlations for each animal for each frequency bin while reported r values reflect the
 664 average r value observed across all rats. Low and high frequency BLP and fEPSP
 665 slope are negatively correlated while these same frequency bins are positively
 666 correlated with PS amplitude. PS amplitude could not be consistently quantified for rat
 667 #7 or #17. For frequency bin labels, “G” = gamma and “B” = beta.

668

669

Infraslow SBA modulates EPSP-PS coupling



670

671 Figure 3. fEPSP slope (A) and PS amplitude (B) as a function of preceding low, middle,
 672 or high frequency BLP quartiles and stimulation frequency (0.25 or 0.10Hz). C)
 673 Average evoked responses from an individual rat for responses following spontaneous
 674 EEG epochs that contained the least (black) and most (grey) BLP for each condition.

675

676

677

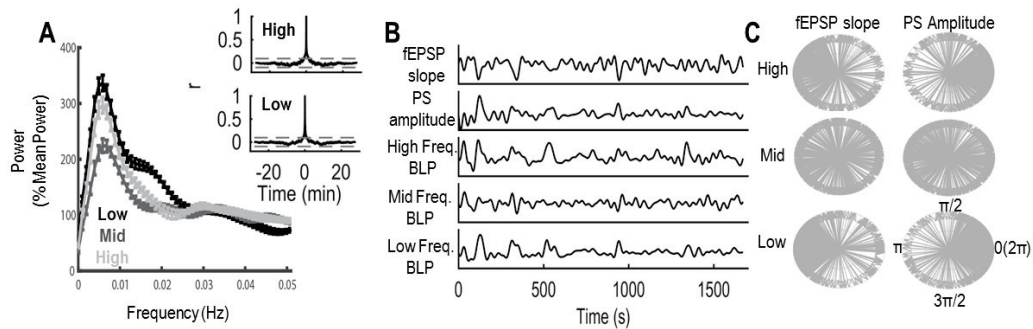
678

679

680

681

Infraslow SBA modulates EPSP-PS coupling



682

683 Figure 4. Phase-locking of EEG BLP, fEPSP slope, and PS amplitudes. A) Average
 684 power spectra (n=17 rats) of low, middle, and high frequency BLP during the entire
 685 power recording session. Insets: Autocorrelograms for infraslow-filtered high and low
 686 frequency BLP. Grey dotted lines depict 95% confidence intervals. B) Spontaneous
 687 fluctuations in evoked response magnitude and EEG BLP are evident in infraslow
 688 filtered time series data from a single rat. C) Instantaneous phase differences
 689 calculated at each data point across the time series data depicted in B. Each grey
 690 arrow represents the phase difference calculated at a single time point. fEPSP and
 691 low/high frequency BLP are typically out of phase (π radians) while PS amplitude and
 692 low/high frequency BLP are typically in phase ($0(2\pi)$ radians). No clear phase locking
 693 is present between middle frequency BLP and fEPSP slope or PS amplitude.

694

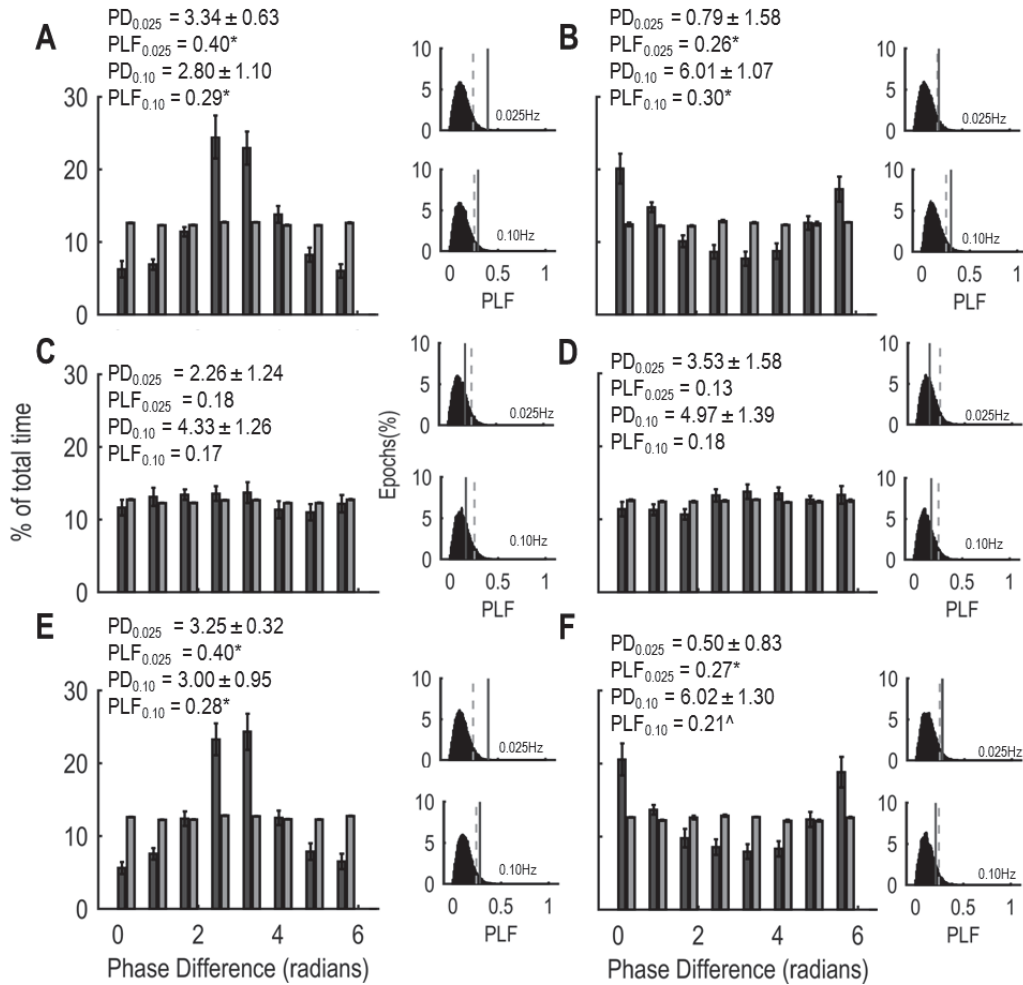
695

696

697

698

Infraslow SBA modulates EPSP-PS coupling

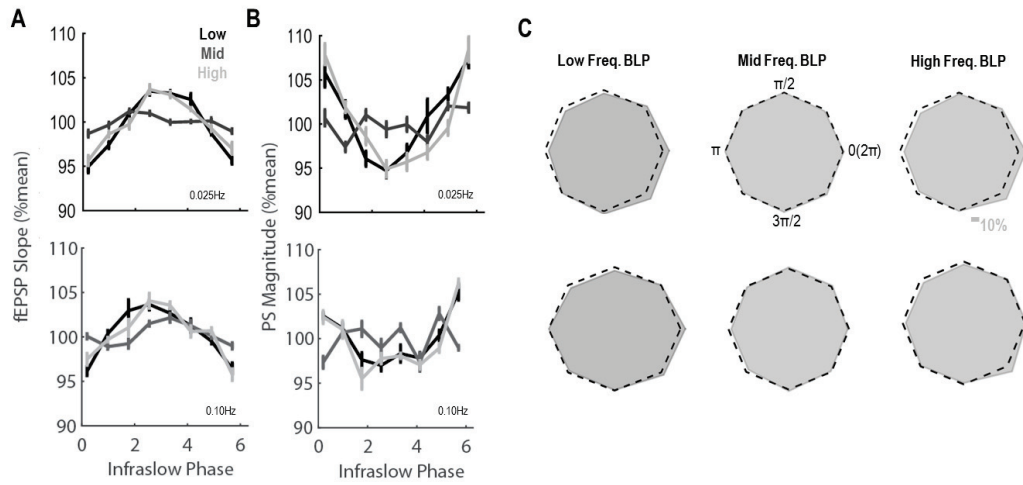


699

700 Figure 5. Instantaneous phase difference between low (A/B), middle (C/D), and high
 701 (E/F) frequency BLP and fEPSP or PS for rats stimulated at 0.25Hz (similar phase
 702 distributions were observed for 0.10Hz stimulated rats). Dark bars depict the
 703 distribution of actual observed phase differences while light bars depict the distribution
 704 of phase differences observed between BLP and shuffled fEPSP or PS data. fEPSP
 705 slopes are predominantly antiphase with high/low BLP while PS amplitudes are
 706 predominantly in phase with high/low BLP. Insets depict the distribution of phase-
 707 locking factors (PLF) calculated between BLP and shuffled fEPSP or PS data
 708 (histogram), the 0.05 critical value obtained from these distributions (dotted line) and the
 709 PLF calculated from observed data (solid grey line). PD = circular mean phase
 710 difference \pm circular standard deviation. Phase locking: * = $p < 0.05$, ^ = $p < 0.10$.

711

Infraslow SBA modulates EPSP-PS coupling



712

713 Figure 6. fEPSP slope (A) and PS amplitude (B) vary as a function of the phase of
 714 infraslow fluctuations in low and high frequency BLP but are not significantly altered by
 715 infraslow changes in middle frequency BLP. C) The opposing effects of infraslow BLP
 716 phase on fEPSP slope and PS amplitude produce variations in EPSP-PS coupling
 717 across infraslow cycles in rats stimulated at either 0.25Hz (top row) or 0.10Hz (bottom
 718 row). Dotted lines depict unitary EPSP-PS coupling at all phases and grey regions
 719 depict observed coupling (regions that exceed dotted lines indicate stronger EPSP-PS
 720 coupling than average while regions that do not reach dotted lines indicate weaker
 721 EPSP-PS coupling). Scale bar represents a change of 10% of the mean EPSP-PS
 722 coupling.

723

724

725

726

727

728

729

730

731

732

733

734 **References**

- 735 Berens P (2009) CircStat: a MATLAB toolbox for circular statistics. *J Stat Softw* 31:1–21.
- 736 Berretta N, Rossokhin AV, Kasyanov AM, Sokolov MV, Cherubini E, Voronin LL (2000) Postsynaptic
737 hyperpolarization increases the strength of AMPA-mediated synaptic transmission at large
738 synapses between mossy fibers and CA3 pyramidal cells. *Neuropharmacology* 39:2288–2301.
- 739 Birbaumer N, Elbert T, Canavan AG, Rockstroh B (1990) Slow potentials of the cerebral cortex and
740 behavior. *Physiol Rev* 70:1–41.
- 741 Bramham C, Srebro B (1989) Synaptic plasticity in the hippocampus is modulated by behavioral state.
742 *Brain Res* 493:74–86.
- 743 Bramham CR (1998) Phasic boosting of medial perforant path-evoked granule cell output time-locked to
744 spontaneous dentate EEG spikes in awake rats. *J Neurophysiol* 79:2825–2832.
- 745 Broyd SJ, Helps SK, Sonuga-Barke EJS (2011) Attention-Induced Deactivations in Very Low Frequency EEG
746 Oscillations: Differential Localisation According to ADHD Symptom Status. *PLoS ONE* 6:e17325.
- 747 Buzsáki G, Draguhn A (2004) Neuronal oscillations in cortical networks. *science* 304:1926–1929.
- 748 Chan AW, Mohajerani MH, LeDue JM, Wang YT, Murphy TH (2015) Mesoscale infraslow spontaneous
749 membrane potential fluctuations recapitulate high-frequency activity cortical motifs. *Nat*
750 *Commun* 6:7738.
- 751 Coenen AM (1975) Frequency analysis of rat hippocampal electrical activity. *Physiol Behav* 14:391–394.
- 752 Colgin LL (2015) Theta–gamma coupling in the entorhinal–hippocampal system. *Curr Opin Neurobiol*
753 31:45–50.
- 754 Daoudal G, Debanne D (2003) Long-term plasticity of intrinsic excitability: learning rules and
755 mechanisms. *Learn Mem Cold Spring Harb N* 10:456–465.
- 756 Deco G, Corbetta M (2011) The Dynamical Balance of the Brain at Rest. *The Neuroscientist* 17:107–123.
- 757 Destexhe A, Rudolph M, Fellous J-M, Sejnowski TJ (2001) Fluctuating synaptic conductances recreate in
758 vivo-like activity in neocortical neurons. *Neuroscience* 107:13–24.
- 759 Faisal AA, Laughlin SB (2007) Stochastic simulations on the reliability of action potential propagation in
760 thin axons. *PLoS Comput Biol* 3:e79.
- 761 Fellous J-M, Rudolph M, Destexhe A, Sejnowski T. (2003) Synaptic background noise controls the
762 input/output characteristics of single cells in an in vitro model of in vivo activity. *Neuroscience*
763 122:811–829.
- 764 Ferguson AL, Stone TW (2010) Glutamate-induced depression of EPSP-spike coupling in rat hippocampal
765 CA1 neurons and modulation by adenosine receptors. *Eur J Neurosci* 31:1208–1218.

Infraslow SBA modulates EPSP-PS coupling

- 766 Filippov IV, Williams WC, Frolov VA (2004) Very slow potential oscillations in locus coeruleus and dorsal
767 raphe nucleus under different illumination in freely moving rats. *Neurosci Lett* 363:89–93.
- 768 Fontanini A, Katz DB (2008) Behavioral States, Network States, and Sensory Response Variability. *J*
769 *Neurophysiol* 100:1160–1168.
- 770 Fox MD, Snyder AZ, Zacks JM, Raichle ME (2005) Coherent spontaneous activity accounts for trial-to-trial
771 variability in human evoked brain responses. *Nat Neurosci* 9:23–25.
- 772 Freund TF, Buzsaki G (1996) Interneurons of the hippocampus. *Hippocampus* 6:347–470.
- 773 Green EJ, McNaughton BL, Barnes CA (1990) Exploration-dependent modulation of evoked responses in
774 fascia dentata: dissociation of motor, EEG, and sensory factors and evidence for a synaptic
775 efficacy change. *J Neurosci* 10:1455–1471.
- 776 He BJ, Raichle ME (2009) The fMRI signal, slow cortical potential and consciousness. *Trends Cogn Sci*
777 13:302–309.
- 778 Henze DA, Wittner L, Buzsaki G (2002) Single granule cells reliably discharge targets in the hippocampal
779 CA3 network in vivo. *Nat Neurosci* 5:790–796.
- 780 Hesselmann G, Kell CA, Eger E, Kleinschmidt A (2008) Spontaneous local variations in ongoing neural
781 activity bias perceptual decisions. *Proc Natl Acad Sci* 105:10984–10989.
- 782 Hsu D (2007) The dentate gyrus as a filter or gate: a look back and a look ahead. In: *Progress in Brain*
783 *Research*, pp 601–613. Elsevier.
- 784 Hyman JM, Wyble BP, Goyal V, Rossi CA, Hasselmo ME (2003) Stimulation in hippocampal region CA1 in
785 behaving rats yields long-term potentiation when delivered to the peak of theta and long-term
786 depression when delivered to the trough. *J Neurosci* 23:11725–11731.
- 787 Jensen O, Colgin LL (2007) Cross-frequency coupling between neuronal oscillations. *Trends Cogn Sci*
788 11:267–269.
- 789 Jetli SK, Vendrell-Llopis N, Yaksi E (2014) Spontaneous Activity Governs Olfactory Representations in
790 Spatially Organized Habenular Microcircuits. *Curr Biol* 24:434–439.
- 791 Jones LM, Fontanini A, Sadacca BF, Miller P, Katz DB (2007) Natural stimuli evoke dynamic sequences of
792 states in sensory cortical ensembles. *Proc Natl Acad Sci* 104:18772–18777.
- 793 Jung MW, McNaughton BL (1993) Spatial selectivity of unit activity in the hippocampal granular layer.
794 *Hippocampus* 3:165–182.
- 795 Kelly AMC, Uddin LQ, Biswal BB, Castellanos FX, Milham MP (2008) Competition between functional
796 brain networks mediates behavioral variability. *NeuroImage* 39:527–537.
- 797 Kitchigina V, Vankov A, Harley C, Sara SJ (1997) Novelty-elicited, Noradrenaline-dependent
798 Enhancement of Excitability in the Dentate Gyrus. *Eur J Neurosci* 9:41–47.

Infraslow SBA modulates EPSP-PS coupling

- 799 Klancnik JM, Phillips AG (1991) Modulation of synaptic plasticity in the dentate gyrus of the rat by
800 electrical stimulation of the median raphe nucleus. *Brain Res* 557:236–240.
- 801 Korol DL, Gold PE (2008) Epinephrine converts long-term potentiation from transient to durable form in
802 awake rats. *Hippocampus* 18:81–91.
- 803 Kuga N, Sasaki T, Takahara Y, Matsuki N, Ikegaya Y (2011) Large-Scale Calcium Waves Traveling through
804 Astrocytic Networks In Vivo. *J Neurosci* 31:2607–2614.
- 805 Leutgeb JK, Leutgeb S, Moser M-B, Moser EI (2007) Pattern separation in the dentate gyrus and CA3 of
806 the hippocampus. *science* 315:961–966.
- 807 Lewis CM, Baldassarre A, Comitteri G, Romani GL, Corbetta M (2009) Learning sculpts the spontaneous
808 activity of the resting human brain. *Proc Natl Acad Sci* 106:17558–17563.
- 809 Lindquist BE, Shuttleworth CW (2012) Adenosine receptor activation is responsible for prolonged
810 depression of synaptic transmission after spreading depolarization in brain slices. *Neuroscience*
811 223:365–376.
- 812 Lisman JE (1999) Relating hippocampal circuitry to function: recall of memory sequences by reciprocal
813 dentate–CA3 interactions. *Neuron* 22:233–242.
- 814 Lőrincz ML, Geall F, Bao Y, Crunelli V, Hughes SW (2009) ATP-Dependent Infra-Slow (0.1 Hz)
815 Oscillations in Thalamic Networks Kleinschnitz C, ed. *PLoS ONE* 4:e4447.
- 816 Mantini D, Perrucci MG, Del Gratta C, Romani GL, Corbetta M (2007) Electrophysiological signatures of
817 resting state networks in the human brain. *Proc Natl Acad Sci* 104:13170–13175.
- 818 McNaughton BL, Barnes CA (1977) Physiological identification and analysis of dentate granule cell
819 responses to stimulation of the medial and lateral perforant pathways in the rat. *J Comp Neurol*
820 175:439–453.
- 821 Mitchell SJ, Rawlins JN, Steward O, Olton DS (1982) Medial septal area lesions disrupt theta rhythm and
822 cholinergic staining in medial entorhinal cortex and produce impaired radial arm maze behavior
823 in rats. *J Neurosci* 2:292–302.
- 824 Monto S, Palva S, Voipio J, Palva JM (2008) Very Slow EEG Fluctuations Predict the Dynamics of Stimulus
825 Detection and Oscillation Amplitudes in Humans. *J Neurosci* 28:8268–8272.
- 826 Moser E, Moser MB, Andersen P (1993) Synaptic potentiation in the rat dentate gyrus during exploratory
827 learning. *Neuroreport* 5:317–320.
- 828 Palva JM, Palva S (2012) Infra-slow fluctuations in electrophysiological recordings, blood-oxygenation-
829 level-dependent signals, and psychophysical time series. *NeuroImage* 62:2201–2211.
- 830 Penttonen M, Kamondi A, Sik A, Acsády L, Buzsáki G (1997) Feed-forward and feed-back activation of the
831 dentate gyrus in vivo during dentate spikes and sharp wave bursts. *Hippocampus* 7:437–450.

Infraslow SBA modulates EPSP-PS coupling

- 832 Penttonen M, Nurminen N, Miettinen R, Sirviö J, Henze DA, Csicsvari J, Buzsáki G (1999) Ultra-slow
833 oscillation (0.025 Hz) triggers hippocampal afterdischarges in Wistar rats. *Neuroscience* 94:735–
834 743.
- 835 Raichle ME (2011) The restless brain. *Brain Connect* 1:3–12.
- 836 Raichle ME (2015) The Brain's Default Mode Network. *Annu Rev Neurosci* 38:433–447.
- 837 Sadaghiani S, Kleinschmidt A (2013) Functional interactions between intrinsic brain activity and
838 behavior. *NeuroImage* 80:379–386.
- 839 Scaglione A, Moxon KA, Aguilar J, Foffani G (2011) Trial-to-trial variability in the responses of neurons
840 carries information about stimulus location in the rat whisker thalamus. *Proc Natl Acad Sci U S A*
841 108:14956–14961.
- 842 Schall KP, Kerber J, Dickson CT (2008) Rhythmic Constraints on Hippocampal Processing: State and
843 Phase-Related Fluctuations of Synaptic Excitability During Theta and the Slow Oscillation. *J*
844 *Neurophysiol* 99:888–899.
- 845 Schmidt-Hieber C, Jonas P, Bischofberger J (2007) Subthreshold Dendritic Signal Processing and
846 Coincidence Detection in Dentate Gyrus Granule Cells. *J Neurosci* 27:8430–8441.
- 847 Schroeder CE, Lakatos P (2009) Low-frequency neuronal oscillations as instruments of sensory selection.
848 *Trends Neurosci* 32:9–18.
- 849 Shirvalkar PR, Rapp PR, Shapiro ML (2010) Bidirectional changes to hippocampal theta-gamma
850 comodulation predict memory for recent spatial episodes. *Proc Natl Acad Sci* 107:7054–7059.
- 851 Smith SM, Fox PT, Miller KL, Glahn DC, Fox PM, Mackay CE, Filippini N, Watkins KE, Toro R, Laird AR,
852 Beckmann CF (2009) Correspondence of the brain's functional architecture during activation and
853 rest. *Proc Natl Acad Sci U S A* 106:13040–13045.
- 854 Sterzer P, Kleinschmidt A, Rees G (2009) The neural bases of multistable perception. *Trends Cogn Sci*
855 13:310–318.
- 856 Vanhatalo S, Palva JM, Holmes MD, Miller JW, Voipio J, Kaila K (2004) Infraslow oscillations modulate
857 excitability and interictal epileptic activity in the human cortex during sleep. *Proc Natl Acad Sci U*
858 *S A* 101:5053–5057.
- 859 Winson J, Abzug C (1977) Gating of neuronal transmission in the hippocampus: efficacy of transmission
860 varies with behavioral state. *Science* 196:1223–1225.
- 861 Wulff P, Ponomarenko AA, Bartos M, Korotkova TM, Fuchs EC, Böhner F, Both M, Tort AB, Kopell NJ,
862 Wisden W, others (2009) Hippocampal theta rhythm and its coupling with gamma oscillations
863 require fast inhibition onto parvalbumin-positive interneurons. *Proc Natl Acad Sci* 106:3561–
864 3566.
- 865 Zsiros V, Hestrin S (2005) Background synaptic conductance and precision of EPSP-spike coupling at
866 pyramidal cells. *J Neurophysiol* 93:3248–3256.

Infraslow SBA modulates EPSP-PS coupling

867 Zylbertal A, Yarom Y, Wagner S (2017) Synchronous Infra-Slow Bursting in the Mouse Accessory
868 Olfactory Bulb Emerge from Interplay between Intrinsic Neuronal Dynamics and Network
869 Connectivity. *J Neurosci* 37:2656–2672.

870

